JOURNAL OF MATERIALS SCIENCE 24 (1989) 139–142

Non-isothermal crystallization and isothermal transformation kinetics of the $Ni_{68.5}Cr_{14.5}P_{17}$ metallic glass

C. F. CONDE, H. MIRANDA, A. CONDE, R. MARQUEZ
Departamento de Física del Estado Sólido, Instituto de Ciencias de Materiales de Sevilla, Universidad de Sevilla-CSIC, Apdo. 1065, Seville 41080, Spain

Non-isothermal crystallization of the $Ni_{68.5}Cr_{14.5}P_{17}$ alloy is characterized by differential scanning calorimetry (DSC) and X-ray techniques. Transformation occurs in two stages at peak temperatures 622 ± 1 and 692 ± 1 K (at 20 K min^{-1}), with ΔH_1 = 1.50 + 0.1 kJ mol^{-1} and ΔH_2 = 3.0 ± 0.1 kJ mol^{-1}. Precipitation of a nickel phase occurs in the first stage and a $(NiCr)_3P$ phase is formed during the second stage. An approach to the isothermal kinetics of the two crystallization events is derived within the frame work of the Johnson–Mehl–Avrami theory.

1. Introduction

Metallic glasses are a new class of materials which are produced in the amorphous state by ultrarapid quenching of the melt. Being metastable, they tend to crystallize at particular combinations of temperature and time. Crystallization deteriorates drastically the remarkable combination of useful properties of these materials and this restricts a broader use of amorphous alloys. So, the investigation of the crystallization behaviour of metallic glasses is important from the technological point of view, as well as purely scientific interest.

Crystallization processes are generally complex and often occur through many stages including intermediate metastable crystalline phases. The thermal stability and the crystallization mechanisms of amorphous alloys depend strongly upon their chemical composition, and, for example, relatively small addition of a third element to the iron-, cobalt- and nickel-metalloid binary alloys generally increase both the crystallization temperature and the activation energy for crystallization [1, 2] but the reason for this effect remains unclear. For iron-, cobalt- and nickel-based metallic glasses containing a second transition metal the stability seems to be related to both the average outer (d + s) electron concentration of the transition metal components and the atomic size difference between solvent and solute metal species [3, 4].

In this paper we report a characterization of the crystallization processes in a chromium containing Ni–P amorphous alloy using differential scanning calorimetry (DSC) and X-ray dffraction methods. Also, an approach to the isothermal kinetics of the crystallization events is derived from isothemal DSC experiments in the framework for the Johnson–Mehl–Avrami theory.

2. Experimental procedure

Glassy ribbons, 25 mm wide and 30 μm thick with nominal composition Ni(balance), Cr(13.0 to 15.0), P(9.7 to 10.5), C(< 0.08) wt % (MBF65 alloy), were kindly supplied by Allied Chemical Corp. Both types of DSC experiments, continuous heating and isothermal annealing, were carried out in a Perkin–Elmer DSC-IIC calorimeter. The temperature and power calibrations of the instrument were checked by using lead and K_2SO_4 standards. Heating rates of 2.5, 5, 10, 20, 40 and 80 K min^{-1} were used in continuous heating experiments. In order to prevent unwanted annealing the specimens – pieces from 2 to 6 mg in weight – were heated to a temperature 100 degrees below the first exotherm at maximum available rate (320 K min^{-1}) from room temperature. For isothermal scans the specimens were also heated to the annealing temperature at the maximum available rate.

The ordinate in both dynamic and isothermal DSC scans is proportional to the net power input to the sample, relative to the power input to a stable reference sample. The instantaneous rate of change of the volume fraction x of transformed material is

$$dx/dt = (1/\Delta H)\, dq/dt$$

where dq/dt is the power, ΔH is the enthalpy of the transformation, and one assumes that the heat per given fraction of the transformation is uniform in time and independent of x. ΔH is obtained from the total area between the transformation curve and a properly constructed baseline. Integration of the experimental isothermal DSC curve from $t = 0$ at the start of transformation to any later time t yields a partial area β, measured in the same units as the total area α, such that $\beta = x\alpha$, since $x = 1$ at completion. Thus the DSC record yields the volume fraction x (t) as the ratio of the corresponding partial area to the total area β/α. The peak areas were measured with an image analyser.

X-ray diffraction spectra were recorded with Cu$K\alpha$ radiation on a Philips diffractometer, at a scanning

0022–2461/89 $03.00 + .12

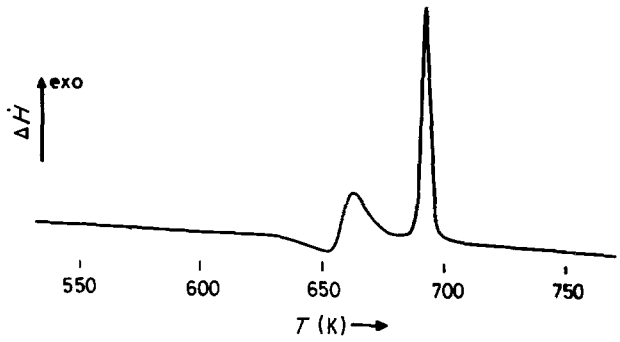

Figure 1 DSC record, at a heating rate of 20 K min^{-1}, showing the two resolved exotherms and the endothermic features associated with T_g.

rate of 2 degrees (2θ) min^{-1}. The working conditions were 40 kV and 20 mA. To allow direct correlation of the phase composition with the calorimetry results, XRD scans were made at room temperature on segments previously heated in the DSC chamber and abruptly cooled to room temperature, by selecting the 320 K min^{-1} cooling rate of the instrument.

3. Non-isothermal crystallization

3.1. Calorimetry

Fig. 1 shows the DSC dynamic scan obtained by continuous heating at a rate of 20 K min^{-1}, under dry argon atmosphere, for a sample of 2.43 mg of as-quenched alloy. The DSC record exhibits exothermic and endothermic effects associated with the sequence of transformation from the glass-to-supercooled liquid-to-polycrystalline multiphase aggregate. Crystallization proceeds by at least two steps as revealed by the two resolved exotherms, occurring at peak temperatures 662 ± 1 and 692 ± 1 K respectively, for a heating rate of 20 K min^{-1}. The enthalpies of transformation derived from the areas under the exotherms are 1.5 ± 0.1 and 3.0 ± 0.1 kJ mol^{-1} respectively, and no significant change in the enthalpy ratio of the two exotherms is observed with the heating rate. A small endothermic effect occurs at temperatures slightly lower (about 20 K) than the first exotherm. These endothermic effects are usually associated with the rapid rise in the specific heat at the glass–supercooled liquid transition [5]. However, in this case (as is generally the case for many metallic glasses) the glass transition is truncated by the start of crystallization and T_g, defined by the temperature for the start of the transition, is 655 K.

A DSC scan of partially crystallized samples showed only the higher temperature exotherm and no trace of the lower temperature exotherm was detected at any rate. The position of the higher temperature DSC peak did not change after the samples were partially crystallized and no other transformation was detected by heating up to 800 K.

The characteristic peak temperatures of the crystallization exotherms for this alloy are appreciably lower than those observed for the $Ni_{63}Cr_{18}Si_{13}B_6$ alloy (747 and 821 K respectively) [6] in spite of a similar metal–metalloid ratio in the composition of both alloys. So, the different chromium content appears to have a significant effect on the thermal stability of the glass,

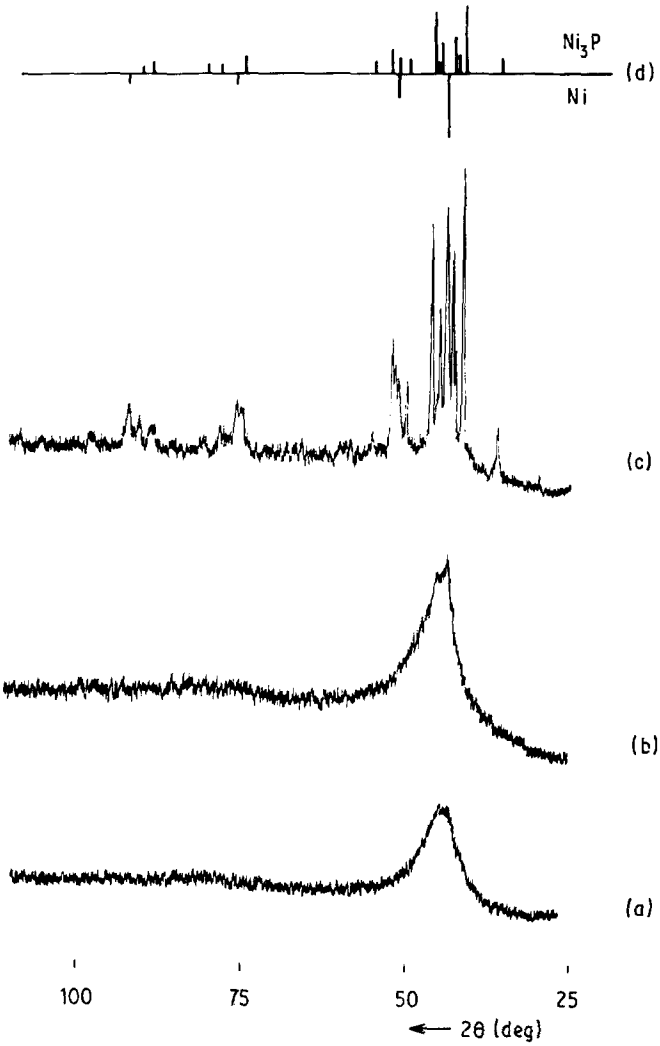

Figure 2 X-ray diffraction records for different heat-treatment samples: (a) as-received ribbon; (b) sample heated at 20 K min^{-1}, up to complete the first exotherms (680 K); (c) sample heated up to the second exotherm (750 K); and (d) characteristic lines for Ni and $(NiCr)_3P$.

in a similar way to that reported for Fe–Cr alloys, in which an increase of crystallization temperature with chromium content is generally observed [7, 8]. Also, the different metalloids contained in these alloys should affect appreciably the crystallization features.

The activation energy of the crystallization events were determined by the Kissinger's peak shift method [9] and the values obtained were 404 ± 10 kJ mol^{-1} (4.2 ± 0.1 eV at^{-1}) for the first stage and 368 ± 10 kJ mol^{-1} (3.8 ± 0.1 eV at^{-1}) for the second crystallization stage.

3.2. X-ray diffraction

Fig. 2 shows the significant portions of diffractometer recording for as-received and heat-treated samples. Under X-ray diffraction analysis, the as-received ribbons exhibited only the broad halo characteristic of amorphous materials at diffraction angles in the range 40 to 50 degrees (2θ) (Fig. 2a), the maximum of which corresponds to the (1 1 1) line of nickel in the crystalline state. For samples partially crystallized in the calorimeter chamber (up to completion of the first exotherm) the existence of a crystalline phase is revealed on diffractograms (Fig. 2b). A narrow diffraction

peak, of low intensity, now appears, its peak maximum position corresponding to the (1 1 1) line of a Ni–Cr solid solution. Also, a broad maximum due to the remaining amorphous phase is observed. Thus, it can be supposed that the initial crystallization stage is connected with the formation of a Ni–Cr crystalline phase coexisting with the still amorphous matrix. The low intensity of the characteristic lines should be related to the small fraction of precipitated crystals. As expected, for samples partially crystallized at higher heating rates a less advanced stage of crystallization is found, as revealed by the number and intensity of resolved lines. Finally, for entirely crystallized samples (annealed at 750 K, beyond the second DSC exotherm) the X-ray pattern (Fig. 2c) showed along with enhanced lines of the Ni–Cr phase, new diffraction lines that can be assigned to a $(Ni, Cr)_3P$ phase. In this second stage the amorphous phase is exhausted, as revealed by the absence of a broad maximum in the X-ray scan.

4. Isothermal kinetics

The generally accepted model for the crystallization kinetics of metallic glasses is the Johnson–Mehl–Avrami (JMA) equation [10]:

$$x(t) = 1 - \exp[-b(t - t_0)^n]$$

where $x(t)$ is the fraction transformed after time t, t_0 is the incubation time, b is a rate constant and n is an exponent which need not be an integer [11]. This exponent reflects the nucleation rate and/or the growth morphology whereas the rate constant depends on both the nucleation rate and the growth rate, b may be expected to exhibit an Arrhenius temperature dependence as

$$b = b_0 \exp(-E/kT)$$

where E is an effective activation energy for the transformation, i.e. for removal of an atom from the amorphous matrix and migration across the interface on to a crystallite or diffusion to a nucleation site.

For isothermal crystallization a plot of $\ln[-\ln(1 - x)]$ against $\ln t$ should give a straight line of gradient n. If the assumptions of spatially random nucleation and linear growth (growth rate not depending on time) are made, two simple cases can be distinguished: $n = 4$ will imply a constant nucleation rate; $n = 3$ will imply a zero nucleation rate, i.e. growth only on pre-existing nuclei. However, when the growth rate is controlled by long-range diffusion processes, values of n in the transformation equation are $n = 5/2$ for a nucleation rate constant and $n = 3/2$ for early site saturation of randomly placed heterogeneous nuclei.

Fig. 3 shows the sigmoidal patterns, typical of JMA transformations, for the two crystallization events derived from isothermal DSC at different annealing temperatures. Each data point is derived from the integrated intensity under the isothermal curve at that temperature as explained in the experimental section. If a ln–ln plot of $-\ln(1 - x)$ against t yields a straight line, one can assume that the transformation is not inconsistent with the JMA theory of transformations. Fig. 4 shows the ln–ln plots for the two crystallization stages with time plotted referred to $t = 0$ at the end of the incubation period. The parameters n and b can be determined from the slope and intercept respectively by linear regression analysis.

For the first crystallization exotherm the experimental x–t data for different annealing temperatures (Fig. 4a) can be roughly fitted to a straight line. The values of the Avrami index n_1 obtained are in the range $2.4 < n_1 < 2.6$ and the correlation coefficients r are higher than 0.995 for all the straight lines. As observed, deviations from the linear fit are more appreciable for high x and it supposes a decrease in n at high x values. An analogous effect has been observed in other metallic glasses and the lowering of n at high x was attributed

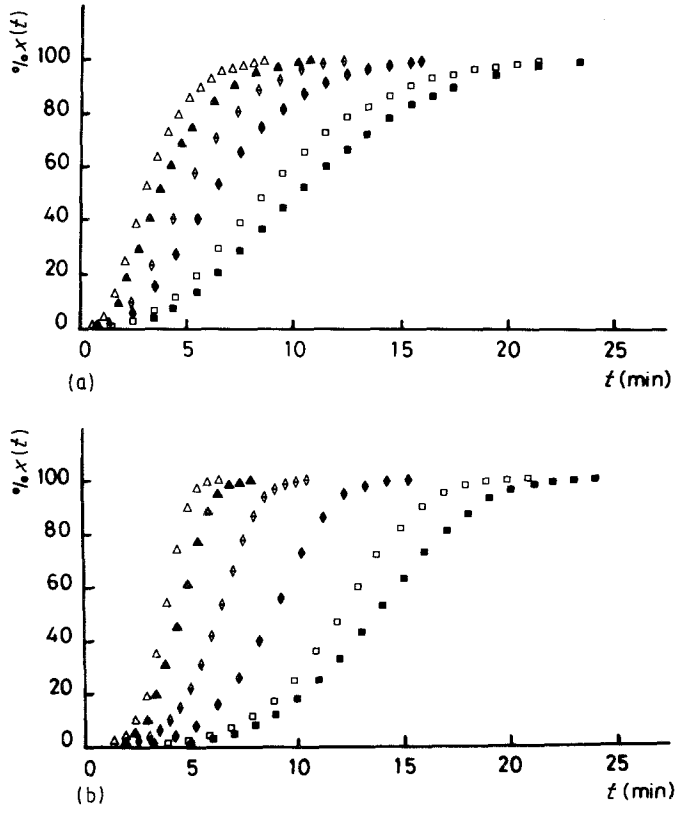

Figure 3 Crystallized fraction plotted against time for different annealing temperatures: (a) first (△ 642 K, ▲ 640 K, ◇ 637 K, ◆ 635 K, □ 632 K, ■ 630 K) and (b) second (△ 655 K, ▲ 662 K, ◇ 660 K, ◆ 655 K, □ 652 K, ■ 650 K) crystallization stages.

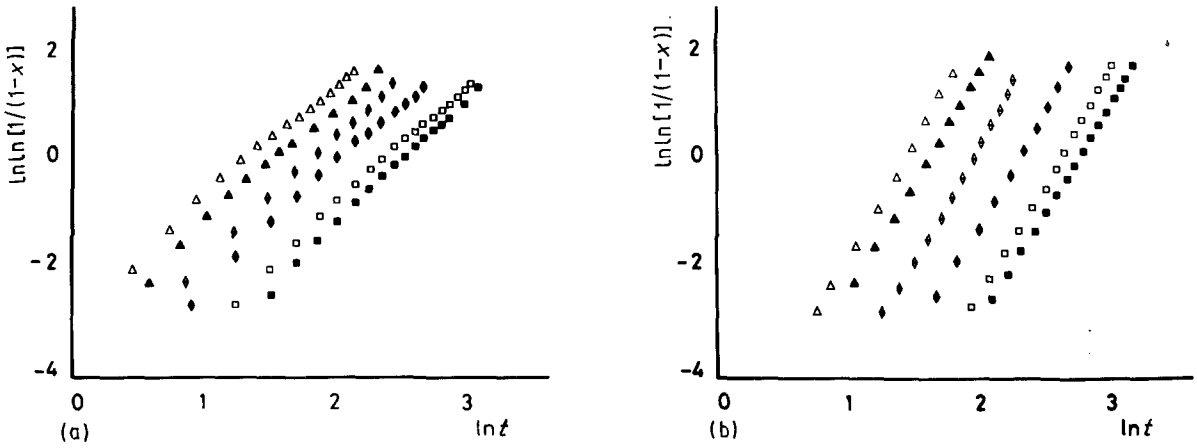

Figure 4 Plots of JMA equations for different isothermal runs: (a) first (△ 642 K, ▲ 640 K, ◇ 637 K, ◆ 635 K, □ 632 K, ■ 630 K) and (b) second (△ 665 K, ▲ 662 K, ◇ 660 K, ◆ 655 K, □ 652 K, ■ 650 K) crystallization stages.

[12, 13] to the delayed crystallization near the rough side of the ribbon. In a similar way, the experimental x–t data of the second crystallization exotherm for different annealing temperatures (Fig. 4b) can be also fitted to a straight line and the values of the Avrami index n_2 are in the range $3.9 < n_2 < 4.1$ ($r > 0.999$ in all cases).

An unambiguous interpretation of the experimental crystallization kinetics, even if only a single phase is involved, is very difficult when microscopic observations are not available, because of the possibiity of several kinds of sites with different nucleation rates and modes of growth. An additional difficulty in the interpretation of the kinetic parameters arises from the presence of two crystalline phases evidenced by the X-ray patterns.

However, it may be helpful to examine the results in the light of an approximate model [14]. Here, it is assumed that $n = a + bp$, where a accounts for the nucleation rate and varies from zero (for quenched-in nuclei) to 1 (for a constant nucleation rate), b defines the dimensionality of the growth ($b = 1, 2$ or 3), p has the value 1 for interfacial control of growth (assumed linear in time), and $p = 0.5$ for diffusion controlled growth.

Thus, the value $n_1 = 2.5$ points to three-dimensional diffusion controlled growth with constant nucleation rate, as expected for primary crystallization. The same value $n_1 = 2.5$ is found for the Avrami index of the first crystallization stage of the analogous NiCrSiB alloy [6]. Values close to 2.5 are also reported for the α-Fe precipitation in the first crystallization step of iron-based metallic glass [13, 15]. For the second crystallization stage the value $n_2 = 4.0$ suggests interface controlled growth with constant nucleation rate. This value of the Avrami index is also obtained for the NiCrSiB alloy [6].

The activation energy for the overall crystallization process can be obtained from either the time taken for a certain fraction of crystallinity read from sigmoidal curves, or from the temperature dependence of the rate constant [10]. A straight line fit of $\ln b$ against $1/T$, as required for the Arrhenius relation, is reasonably well achieved for both exotherms ($r = 0.999$ and $r = 0.997$ respectively) and the slopes yield values of $315 \pm 10\,\mathrm{kJ\,mol^{-1}}$ ($3.3 \pm 0.1\,\mathrm{eV\,at^{-1}}$) and $320 \pm 10\,\mathrm{kJ\,mol^{-1}}$ ($3.3 \pm 0.1\,\mathrm{eV\,at^{-1}}$) for the activation energy of the first and the second crystallization events, respectively. These activation energies obtained from isothermal kinetics do not agree with those obtained by Kissinger's method for the non-isothermal processes.

In conclusion, the $Ni_{68.5}Cr_{14.5}P_{17}$ alloy crystallizes in two stages. In the first one, precipitation of a Ni–Cr phase occurs whereas in the second one the remaining amorphous matrix is transformed to give a $(NiCr)_3P$ phase. So, two crystalline phases, Ni–Cr and $(Ni, Cr)_3P$, coexist in fully crystallized samples. The kinetics of the isothermal crystallization is consistent with the JMA theory and overall activation energies are reported. A model for nucleation and growth mechanisms is suggested on the basis of a simple approach but unambiguous characterization of crystallization events and their complete kinetic description requires microscopic observations, which are contemplated.

References

1. H. J. GUNTHERODT and H. BECK (eds), "Glassy Metals" (Springer, Berlin, 1983).
2. J. L. WALTER, *Mater. Sci. Engng* **50** (1981) 137.
3. I. W. DONALD and H. A. DAVIES, *Phil. Mag. A* **42** (1980) 277.
4. *Idem., Met. Sci.* **16** (1982) 254.
5. D. TURNBULL, *Trans. Met. Soc. AIME* **221** (1961) 422.
6. M. MILLAN, A. CONDE and R. MARQUEZ, to be published.
7. H. J. V. NILSEN, *J. Magn. Magn. Mater.* **12** (1979) 187.
8. R. A. DUNLAP, J. E. BALL and K. DINI, *J. Mater. Sci. Lett.* **4** (1985) 773.
9. H. E. KISSINGER, *Anal. Chem.* **29** (1957) 1702.
10. J. W. CHRISTIAN, "The Theory of Transformations in Metals and Alloys", 2nd Edn (Pergamon, London, 1975) p. 15.
11. M. G. SCOTT, "Amorphous Metallic Alloys", edited by F. E. Luborsky, (Butterworths, London, 1983) p. 162.
12. A. S. SCHAAFSMA, H. SNIJDERS, F. VAN DER WOUDE, J. W. DRIJVER and R. RADELAAR, *Phys. Rev.* **B20** (1979) 7612.
13. H. MIRANDA, C. F. CONDE, A. CONDE and R. MARQUEZ, *Mater. Lett.* **4** (1986) 442.
14. V. R. V. RAMANAN and G. FISH, *J. Appl. Phys.* **53** (1982) 2273.
15. E. G. BABURAJ, G. K. DEY, M. J. PATNI and R. KRISHNAN, *Scripta Metall.* **19** (1985) 305.

Received 28 May
and accepted 16 December 1987